Novel Combined Power and Cooling Thermodynamic Cycle for Low Temperature Heat Sources, Part I: Theoretical Investigation

Article *in* Journal of Solar Energy Engineering · May 2003

DOI: 10.1115/1.1564576

4 authors, including:

D. Yogi Goswami
University of South Florida
484 PUBLICATIONS **7,072** CITATIONS
SEE PROFILE

Afif Hasan
Birzeit University
30 PUBLICATIONS **837** CITATIONS
SEE PROFILE

Novel Combined Power and Cooling Thermodynamic Cycle for Low Temperature Heat Sources, Part I: Theoretical Investigation

Gunnar Tamm
e-mail: gunnar@ufl.edu

D. Yogi Goswami
e-mail: goswami@ufl.edu

Shaoguang Lu

Department of Mechanical Engineering,
University of Florida,
P.O. Box 116300,
Gainesville, FL 32611-6300

Afif A. Hasan
Department of Mechanical Engineering,
Birzeit University,
P.O. Box 14, Birzeit,
Palestinian Authority, Via Israel

A combined thermal power and cooling cycle proposed by Goswami is under intensive investigation, both theoretically and experimentally. The proposed cycle combines the Rankine and absorption refrigeration cycles, producing refrigeration while power is the primary goal. A binary ammonia-water mixture is used as the working fluid. This cycle can be used as a bottoming cycle using waste heat from a conventional power cycle or as an independent cycle using low temperature sources such as geothermal and solar energy. Initial parametric studies of the cycle showed the potential for the cycle to be optimized for first or second law efficiency, as well as work or cooling output. For a solar heat source, optimization of the second law efficiency is most appropriate, since the spent heat source fluid is recycled through the solar collectors. The optimization results verified that the cycle could be optimized. Theoretical results were extended to include realistic irreversibilities in the cycle, in preparation for the experimental study.
[DOI: 10.1115/1.1564576]

Introduction

Multi-component working fluids in power cycles exhibit variable boiling temperatures during the boiling process, which make them suitable for a sensible heat source [1,2]. The temperature difference between the heat source and the working fluid remains small to allow for a good thermal match between the source and working fluid, such that less irreversibility results during the heat addition process.

A novel ammonia-water thermodynamic cycle, capable of producing both power and refrigeration, has been proposed by Goswami [3]. The cycle can alternatively use hydrocarbon mixtures, although a recent study of several combinations of these has not yet shown much promise. An ammonia-water mixture is used as it exhibits desirable thermodynamic properties in terms of a large heat capacity and difference in fluid boiling points in the range of interest. Ammonia is relatively inexpensive, can accommodate system design modifications well, and separates easily from internal lubricating oils [4]. Although ammonia is toxic and hazardous, it is more environmentally friendly than other working fluids.

A schematic of the cycle is shown in Fig. 1. The relatively strong basic solution of ammonia-water leaves the absorber as saturated liquid at the cycle low pressure. It is pumped to the system high pressure and is preheated before entering the boiler by recovering heat from the weak solution returning to the absorber. As the boiler operates between the bubble and dew point temperatures of the mixture at the system high pressure, partial boiling produces a high concentration saturated vapor and relatively low concentration saturated liquid. The liquid weak solution gives up heat in the recovery unit and throttles into the absorber. The rectifier condenses out water to further purify the vapor, by rejecting heat to a secondary strong solution stream, before entering the boiler. The vapor is superheated and expanded through the turbine to produce work. Due to the low boiling point of ammonia the vapor expands to low temperatures yielding the potential for refrigeration. The vapor is finally absorbed back into the liquid, giving off heat as the cycle heat output. Typical values for the properties at the numbered state points can be found in [6–8].

The main parameters that can be varied to influence the cycle are the heat source temperature and flow rate, system high pressure, basic solution ammonia mass fraction, and absorber pressure and temperature. Saturation in the absorber reduces the number of independent main parameters to five that govern the cycle. Recti-

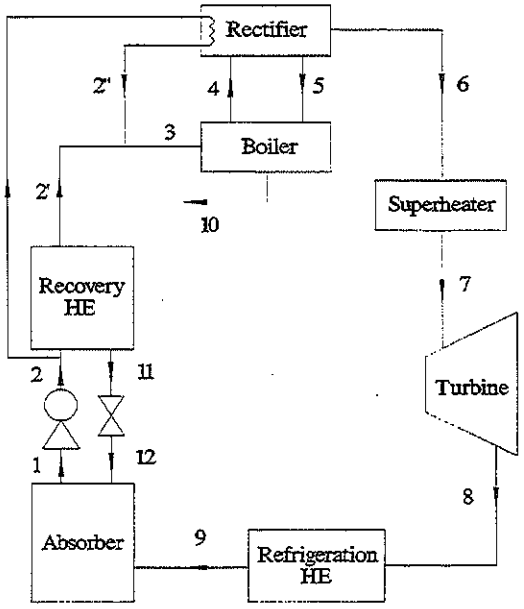

Fig. 1 Schematic of the power and cooling cycle, as used in the theoretical studies

Contributed by the Solar Energy Division of THE AMERICAN SOCIETY OF MECHANICAL ENGINEERS for publication in the ASME JOURNAL OF SOLAR ENERGY ENGINEERING. Manuscript received by the ASME Solar Energy Division, June 2002; final revision, January 2003. Associate Editor: K. Den Braven.

fier and superheater temperatures can also be modified, and the conditions of heat transfer from the source to the ammonia-water mixture can as well.

The cycle can be driven by different heat sources including solar, geothermal, and low temperature waste heat. The use of mid- and low-temperature solar collectors to drive the combined cycle was investigated by Goswami and Xu [5], while using geothermal energy as a heat source was analyzed by Goswami et al. [6].

Typical working conditions of a 400-K boiler temperature superheated to 410 K, and an ambient at 280 K yields a first law efficiency of 23.5%. In comparison, the Carnot efficiency is 31.7% in operating between reservoirs at 410 and 280 K. Conventional power cycles, if operating between the same temperatures, would have lower first-law efficiencies. At higher temperatures, their thermal efficiencies are better in comparison. However, the strength of this cycle lies in the improved heat source utilization. It exhibits much higher second law efficiencies than conventional power cycles.

Property Evaluation

There are several studies on the evaluation of ammonia-water mixture properties in the literature. A convenient semi-empirical scheme is used here that combines the Gibbs free energy method for mixtures and the bubble and dew point temperature correlations for phase equilibrium. The calculated results have been compared to experimental mixture properties in the literature with good agreement [7].

Parametric Analysis. Operating conditions were individually varied in a straightforward parametric analysis to study the effects on the energy transfers and efficiencies of the power and cooling cycle [5]. The parametric analysis gave insight into the behavior of the cycle and showed that optimization of the cycle would be possible for first or second law efficiency, as well as work or cooling output. Figure 2 is a sample of the parametric study, showing a peak in thermal efficiency within the range of operation.

The cycle first-law or thermal efficiency is typically defined as the useful energy output divided by the total energy input, given by Eq. (1).

$$\eta_1 = \frac{W_{net} + Q_c}{Q_h} \tag{1}$$

The net work includes both the turbine output and pump input. Q_c is the refrigeration capacity and Q_h is the total heat added to the cycle from the heat source in both the boiler and superheater. These are calculated based on simple mass and energy balances over the cycle components.

This definition for first law efficiency can be deceiving, as the available energy in refrigeration is less than that in work. Addition of work and cooling output in a single cycle is not documented in the literature, as such a combined cycle is a new idea. Finding and justifying an appropriate definition for first- and second-law efficiencies including both work and cooling is a new concept and is being explored as motivated by this cycle.

A first comparison can be made by scaling the refrigeration term with the *COP* of a refrigeration cycle operating between the appropriate temperatures. The refrigeration term essentially becomes the power required to produce that refrigeration. The Carnot *COP* is used as a limit, although typically the *COP* is much lower at about 3. Equation (2) gives a modified first law efficiency if power output is the primary goal and Eq. (3) can be considered as a new cooling efficiency or coefficient of performance, if refrigeration is the desired output. The power term in Eq. (3) likewise becomes the equivalent refrigeration that could be produced by that input of power with the given refrigeration cycle *COP*.

$$\eta_{1,power} = \frac{W_{net} + Q_c / COP_{refrig}}{Q_h} \tag{2}$$

$$COP_{cycle} = \frac{W_{net} COP_{refrig} + Q_c}{Q_h} \tag{3}$$

Figure 2 shows that for higher ammonia mass fractions in the basic solution, more vaporization occurs for the given boiler temperature and pressure. The optimization has shown that even higher basic solution ammonia mass fractions are desirable. A higher vapor fraction allows for greater flow through the turbine and more work production for a higher thermal efficiency. Note that work and refrigeration here are taken as equivalent, according to Eq. (1), although the trends are similar in using Eqs. (2) or (3). Figure 3 concludes that more vapor is available for refrigeration

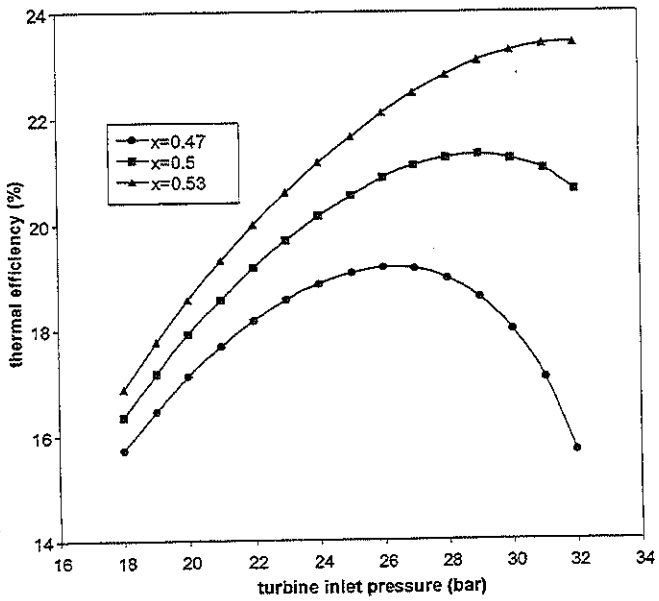

Fig. 2 Effect of turbine inlet pressure on the thermal efficiency (%) of the cycle

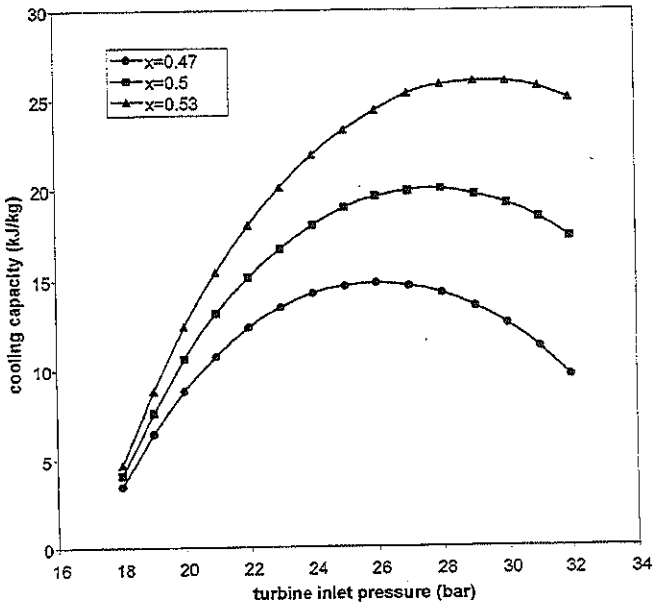

Fig. 3 Effect of turbine inlet pressure on the cooling capacity (kJ/kg) of the cycle

output also, per kg of basic solution that is boiled.

For increasing turbine inlet or system high pressure, the figures show that the work and cooling outputs peak. Determining the location of these peaks is necessary a priori to optimize a working system's performance. The effect of the higher pressure limiting vapor production begins to dominate as the boiler exit fluid is shifted towards saturated liquid. The peak shifts for higher basic solution ammonia mass fractions as a two-phase equilibrium can be sustained at higher pressures for higher ammonia mass fractions.

Figures 2 and 3 were evaluated for a boiler at 400 K, superheater at 410 K, absorber at 280 K, and rectifier at 360 K. The low pressure in the system at the absorber was set at 2 bar. Note that a series of similar plots can be determined by changing any of the operating parameters. Each plot could conceivably provide a visual location of the optimum over the range of interest for the single parameter. For practical operation, the cycle has several parameters that are varied together, presenting a multidimensional surface on which an optimum can be found. A mathematical approach at locating this optimum is suggested.

Optimization

For a solar heat source, optimization of the cycle for maximum second law efficiency is most appropriate as the heat source fluid is recycled back to the solar collectors at a temperature that is higher than the ambient. The unused exergy is not wasted.

Exergy, or availability, is defined as the maximum reversible work a substance can do during the process of reaching equilibrium with its environment. The second law efficiency is defined as the exergy output divided by the exergy input to the cycle [8]. The exergy input is taken as the exergy change of the heat source. The exergy output is the exergy of the net work and the exergy of the refrigeration. The second-law or exergy efficiency is given by Eq. (4).

$$\eta_2 = \frac{W_{net} + E_c}{\Delta E_{hs}} \tag{4}$$

The exergy of refrigeration, E_c, is the refrigeration capacity divided by the coefficient of performance of a Carnot refrigeration cycle operating between the ambient and cycle low temperatures, as given by Eq. (5) [9].

$$E_c = Q_c \frac{(T_0 - T_c)}{T_c} \tag{5}$$

Optimization Methodology. The optimization scheme, as presented by Goswami et al. [6], searches over eight free variables for the optimal second law efficiency as defined by Eq. (4). The parameters are the absorber or ambient temperature, boiler, superheater and rectifier temperature, the boiler pressure (high pressure), absorber pressure (low pressure), and heat source inlet and exit temperatures. From these eight free variables, all other state points in the cycle can be determined with minimal and reasonable assumptions.

Optimization Results. The desired heat source temperature will vary according to the intended use of the cycle. The effects of the heat source temperature on the optimized cycle performance are shown in Figs. 4–7, optimized for second law efficiency. The refrigeration as a fraction of the heat addition, Q_c/Q_h, changes little as the heat source temperature increases as shown in Fig. 4. As the heat source temperature approaches the ambient temperature, refrigeration approaches zero. The highest refrigeration fraction is near a source temperature of 390 K. The refrigeration fraction decreases to zero near 480 K, as the higher temperature vapor can no longer be expanded to sub-ambient temperatures.

The net power as a fraction of heat addition, W_{net}/Q_h, increases as the heat source temperature increases. As the turbine work output is related mainly to the pressure ratio across the turbine, the net power curve can be explained in relation to the pressure ratio in Fig. 5, which shows a continuous increase with the heat source temperature.

The first law efficiency curve, which is a sum of the refrigeration and power curves, shows similar behavior to the power curve up to the maximum value of 23.6% at 400 K. After the maximum point the efficiency starts decreasing slowly in a similar manner to the refrigeration curve. Eq. (1) was used as the first law efficiency definition in Fig. 4, with the magnitude of the curve somewhat reduced if using Eqs. (2) or (3), depending on the *COP* that is used.

The second law or exergy efficiency shows a maximum value of 65.2% at 380 K. The sharp increase in Fig. 4 of the second law efficiency between 320 and 380 K is due to the increase of both power and refrigeration outputs. The second law efficiency reaches a maximum where the refrigeration output begins to decrease above 400 K.

Figure 6 shows the refrigeration to net power ratio versus heat source temperature. In the temperature range between 320 and 360 K this ratio changes rapidly, while above 360 K the ratio decreases slowly, reaching 0.12 at 460 K. Thus, increasing the heat source temperature favors production of power rather than refrigeration.

Figure 7 shows normalized exergy destruction in the cycle as a function of the heat source temperature. The total exergy destruction in the cycle increases with an increase in the heat source temperature. It can be seen in Fig. 7 that the exergy destruction in both the absorber and heat exchanger changes little as the source

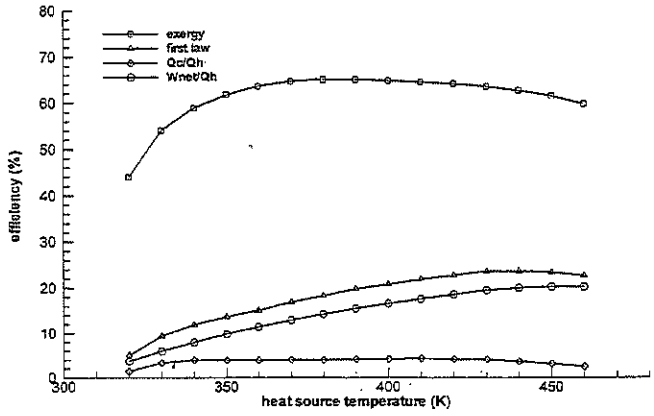

Fig. 4 Efficiencies of the optimized cycle at various heat source temperatures, optimized for second-law efficiency

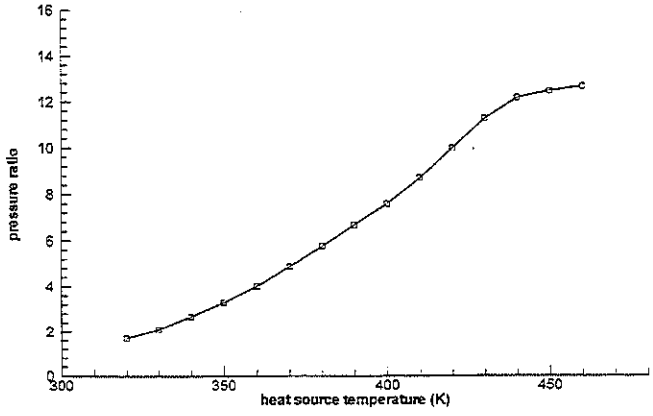

Fig. 5 Pressure ratio of the optimized cycle at various heat source temperatures, optimized for second law efficiency

temperature increases. The superheater has almost no exergy destruction because of its small heat load. The boiler exergy destruction is much lower than that of the absorber.

Exergy destruction in the rectifier increases throughout, as the heating load also increases in the rectifier. The sharp increase is due to more rectification needed for higher heat sources temperatures in order to obtain a high purity vapor stream and thus refrigeration. At even higher temperatures, it becomes too costly to produce refrigeration from a second law efficiency standpoint, such that for optimized cases there is less refrigeration according to Fig. 4. Figure 7 shows that there is less rectification and thus fewer losses in the rectifier.

From the exergy analysis, if the heat source is between 320 and 460 K, then the best operating heat source temperature is around 380 K, since it gives the maximum exergy efficiency. It has been shown that the cycle can be optimized for a range of heat source temperatures. Similarly, the cycle can be optimized for each heat sink or ambient temperature, and other parameters. Therefore the cycle can be customized to the intended application for optimal performance.

Irreversibility Analysis

In realistic systems, there are irreversibilities associated with every component as with this ammonia-water cycle. These irreversibilities will have negative effects on the performance of the cycle. The effects of each loss were studied individually and jointly on the cycle performance. Typical working conditions used in this analysis were 400 K and 30 bar at the boiler exit, 360 K rectification, 410 K at the turbine inlet, 280 K and 2 bar in the absorber, and a basic solution ammonia mass fraction of 0.53.

A typical turbine efficiency of 90% was assumed as suggested in the literature [10]. The thermal efficiency drops from 23.3% to 19.7%, a decrease of 15.4%. Although the pressure ratio is the same, the exhaust temperature of the turbine is higher due to the irreversibility in the turbine. Less energy is converted into mechanical work in the turbine, and the work output drops from 76.1 kW to 68.5 kW, a decrease of 10.0%. At the same time, a higher turbine exhaust temperature provides less cooling capacity. The cooling capacity drops 29.2% from 26.0 kW to 18.4 kW.

An 80% pump efficiency was assumed as suggested in the literature [10]. The pump work requirement increases from 3.4 kW to 4.2 kW. This small increase causes the thermal efficiency to drop slightly.

A pressure loss of 5% of the inlet pressure was assumed across the boiler as suggested in the literature [11]. The results show this pressure loss has almost no negative effect on the cycle performance. Only slightly more pump work is required to boost the boiler inlet pressure to compensate for the pressure loss in the boiler.

A pressure loss of 5% was assumed for the superheater [11]. The results show only a minor negative effect on the cycle performance. Thermal efficiency decreases by 3% of that in the ideal cycle, from 23.3% to 22.6%. Due to the pressure loss in the superheater, the turbine inlet pressure drops. Therefore, less expansion is possible, producing 1.2% less work and higher exhaust temperatures. The cooling capacity decreases by 6.5%.

A pressure loss of 5% was assumed for both streams in the recovery heat exchanger [11]. The effects on the cycle performance are minimal, with a negligible decrease in thermal efficiency owing to an increase in the pump work requirement.

A pressure loss of 5% was assumed in the refrigeration heat exchanger, for comparison to other component pressure losses. The thermal efficiency drops by 2.6% from 23.3% to 22.7%, as the higher turbine exhaust pressure limits the expansion possible. The work output decreases by 1.6%. The reduced turbine pressure ratio also raises the exhaust temperature, reducing the cooling capacity by 4.6%. In a typical cooler, however, the heat exchanger experiences a 3% pressure loss [11], which is the value used in the combined irreversibility study.

Finally, the overall effect of the irreversibility associated with the cycle was analyzed for combined losses. The thermal efficiency decreases by 20.6%, from 23.3% under ideal conditions to 18.5%. The turbine work output drops by 11.8%, from 76.1 kW to 67.1 kW. The cooling capacity decreases by 37.7%, from 26.0 kW to 16.2 kW. It can be seen that the greatest loss is attributed to the expansion in the turbine not being isentropic.

Conclusions

Parametric analysis of the cycle showed the potential for the cycle to be optimized. Optimization of the operating parameters in the cycle is possible for each heat source and heat sink temperature. The cycle may be optimized for the first-law efficiency; second-law efficiency; power output or cooling output, depending on the intended application; and the heat source. In domestic use, this cycle can provide the power and cooling requirement for the home. On an industrial power production scale, the cooling can likewise be used for comfort cooling or a process cooling requirement. For a solar heat source, optimization for the second law efficiency is most appropriate, since the spent heat source fluid is recycled back to the solar collectors. It is found from simulation that optimization of the cycle for second-law efficiency produces no refrigeration at high heat source temperatures, while for low heat source temperatures it does. Inclusion of realistic losses in the analysis of the cycle reduces the cycle thermal efficiency by 20.6%, with 11.8% less work output and 37.7% less cooling ca-

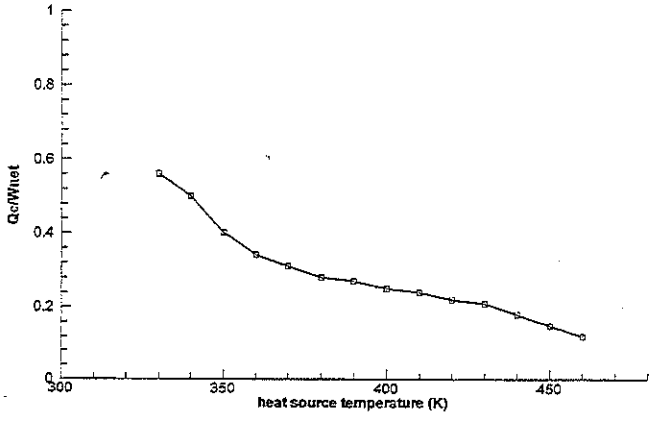

Fig. 6 Ratio of refrigeration to work of the optimized cycle at various heat source temperatures, optimized for second-law efficiency

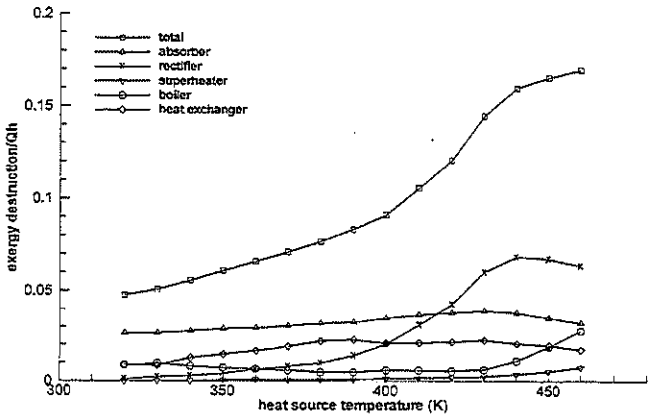

Fig. 7 Exergy destruction of the optimized cycle at various heat source temperatures, optimized for second-law efficiency

pacity. The most significant source of irreversibility in the cycle is a non-isentropic expansion process in the turbine.

Acknowledgment

The authors acknowledge funding from the U.S. Department of Energy for work conducted at the University of Florida.

Nomenclature

COP_{cycle} = equivalent coefficient of performance of the cycle, with work scaled to cooling
COP_{refrig} = coefficient of performance of a refrigeration cycle
E_c = exergy of refrigeration
Q_c = cooling capacity at the refrigeration heat exchanger
Q_h = total heat addition from the boiler and superheater
T_0 = ambient temperature
T_c = refrigeration temperature obtained after expansion
W_{net} = net work output from the turbine and pump
x = basic solution mass fraction of ammonia
ΔE_{hs} = change in exergy of the heat source
η_1 = first law or thermal efficiency
$\eta_{1,power}$ = first law efficiency of the cycle, with cooling scaled to work
η_2 = second law or exergy efficiency

References

[1] Ibrahim, O. M., and Klein, S., 1996, "Absorption Power Cycles," Energy (Oxford), **21**, pp. 21–27.
[2] Kalina, A. I., 1984, "Combined Cycle System With Novel Bottoming Cycle," ASME J. Eng. Gas Turbines Power, **106**, pp. 737–742.
[3] Goswami, D. Y., 1998, "Solar Thermal Technology: Present Status and Ideas for the Future," Energy Sources, **20**, pp. 137–145.
[4] Norton, E., 2001, "Ammonia Liquid Recirculation," ASHRAE J., **43**, 10, pp. 50–51.
[5] Goswami, D. Y., and Xu, F., 1999, "Analysis of a New Thermodynamic Cycle for Combined Power and Cooling Using Low and Medium Temperature Solar Collector," ASME J. Sol. Energy Eng., **121**, pp. 91–97.
[6] Goswami, D. Y., Hasan, A. A., Lu, S., and Tamm, G., 2001, "Ammonia-Based Combined Power/Cooling Cycle," UFME/SEECL Report 2001-05, Univ. of Florida, Gainesville, FL.
[7] Xu, F., and Goswami, D. Y., 1999, "Thermodynamic Properties of Ammonia Water Mixtures for Use in Power Cycles," Energy (Oxford), **24**, pp. 525–536.
[8] Cengel, Y. A., and Boles, M. A., 1998, *Thermodynamics: An Engineering Approach, 3rd Edition*, McGraw-Hill Inc., New York.
[9] Szargut, J., Morris, D. R., and Steward, F. R., 1988, *Exergy Analysis of Thermal, Chemical, and Metallurgical Processes*, Hemisphere Publishing Co., New York, pp. 7–39.
[10] Drbal, L. F., Boston, P. G., Westra, K. L., and Erickson, R. B., 1996, *Power Plant Engineering*, Chapman & Hall, New York.
[11] Bhatt, M. S., Srinivasan, K., Krishna, M. V., and Seetharamu, S., 1994, "Absorption-Resorption Heating Cycles With the New Working Pairs R21-NMP and R21-DMA," Energy Convers. Manage., **35**, pp. 443–451.